Luminescence of Tb^{3+}/Eu^{3+} codoped $LiYF_4$ single crystals under UV excitation for white-light LEDs

Yongzhang Jiang (姜永章)[1], Haiping Xia (夏海平)[1,*], Shuo Yang (杨 硕)[1], Jiazhong Zhang (张加忠)[1], Dongsheng Jiang (江东升)[1], Cheng Wang (王 成)[1], Zhigang Feng (冯治刚)[1], Jian Zhang (张 健)[1], Xuemei Gu (谷雪梅)[1], Jianli Zhang (章践立)[1], Haochuan Jiang (江浩川)[2], and Baojiu Chen (陈宝玖)[3]

[1]*Key Laboratory of Photo-Electronic Materials, Ningbo University, Ningbo 315211, China*
[2]*Ningbo Institute of Materials Technology and Engineering, Chinese Academy of Sciences, Ningbo 315211, China*
[3]*Department of Physics, Dalian Maritime University, Dalian 116026, China*
**Corresponding author: hpxcm@nbu.edu.cn*

Received January 7, 2015; accepted April 29, 2015; posted online June 1, 2015

The absorption spectra, excitation spectra, and emission spectra of Tb^{3+}/Eu^{3+} ions in $LiYF_4$ single crystals synthesized by an improved Bridgman method are measured. The emission spectra of several bands, mainly located at blue ~487 nm ($Tb:{}^5D_4 \rightarrow {}^7F_6$), yellowish green ~542 nm ($Tb:{}^5D_4 \rightarrow {}^7F_5$), and red ~611 nm ($Eu:{}^5D_0 \rightarrow {}^7F_2$) wavelengths, are observed under excitation by UV light. An ideal white light emission as a result of simultaneous combination of these emissions can be obtained from 1.11 mol% Tb^{3+} and 0.9 mol% Eu^{3+} co-doped $LiYF_4$ single crystals with chromaticity coordinates of $x = 0.3242$, $y = 0.3389$, color temperature $T_c = 5878$ K, color rendering index $R_a = 77$, and color quality scale $Q_a = 75$ under excitation of 384 nm light. The chromaticity coordinate, color rendering index, and color quality scale can be modified by the change of the concentration of rare-earth dopants and the excitation wavelength.

OCIS codes: 160.0160, 230.0230, 300.0300.
doi: 10.3788/COL201513.071601.

Recently, a significantly increasing interest has been drawn from rare-earth (RE) ion doped single-host full-color emitting solid state materials for achieving white light emission because they show superior properties such as high heat resistance, high luminous efficiency, low light scattering, and low power consumption which could overcome the weaknesses of using the common two commonly used methods to obtain white LEDs[1–3].

So far, a lot of work has been carried out on the possible application of RE ions such as Tb^{3+}/Sm^{3+}, Eu^{3+}/Dy^{3+}, $Ce^{3+}/Tb^{3+}/Sm^{3+}$, and $Tm^{3+}/Dy^{3+}/Sm^{3+}$ doped transparent solid-state materials in white LEDs[4–8]. As is well-known, under UV light excitation, Tb^{3+} ions have transitions in the blue light region ~487 nm ($^5D_4 \rightarrow {}^7F_6$) and yellowish-green light region ~542 nm ($^5D_4 \rightarrow {}^7F_5$), while Eu^{3+} ions can emit red light ~611 nm ($^5D_0 \rightarrow {}^7F_2$)[9–12]. These full-color emissions including blue-, green-, and red-emitting light could potentially enable a near-ideal white light. Tb^{3+}/Eu^{3+} ions co-doped glasses have been fabricated and white emitting light was obtained[10,12].

Besides the dopants of REs, the host material also plays a significant role in LED applications. Previous LED materials mainly focused on glasses[6,7], glass ceramics[4,5], and transparent ceramics[8]. Single crystals can be considered to be very favorable as the host materials for optical devices because they have high luminous efficiency, high mechanical strength, and excellent chemical durability. Recently, we prepared $LiYF_4$ single crystals co-doped with Tm^{3+}/Dy^{3+}, and Dy^{3+} for a white light emission[3,13]. The single crystals have advantages of excellent thermal and mechanical properties, better transmittance, superior radiation resistance, as well as higher luminous efficiency. However, there are only a few reports about Tb^{3+}/Eu^{3+} co-doped single crystals for white LED applications. In this Letter, a $LiYF_4$ single crystal co-doped with Tb^{3+}/Eu^{3+} was obtained by the modified Bridgman method, and the luminescence properties of the crystal were characterized, aimed at using it as a new potential host material for white LED applications.

$LiYF_4$ single crystals doped with Tb^{3+} and co-doped with Tb^{3+}/Eu^{3+} were successfully synthesized by a vertical Bridgman method. High-purity LiF, YF_3, TbF_3, and EuF_3 as feed materials without any preprocessing were prepared for crystals growth. The Li-rich composition could be beneficial for the growth of these transparent crystals. The molar composition of the single crystals was determined by the formulas $LiY_{0.991}Tb_{0.009}F_4$ and $LiY_{1-x-y}Tb_xEu_yF_4$ ($x = 0.009$, 0.010, 0.011, 0.011, and 0.011; $y = 0.008$, 0.008, 0.008, 0.010, and 0.012, respectively). Then the as-prepared mixture of raw materials was ground ~1 h in a mortar. The moisture and the some oxygen impurities in the fluoride powders were removed completely using the high-temperature hydrofluorination method by which the powders were sintered with anhydrous HF at 800°C for 8 h. The as-produced polycrystalline bars were fully ground in a mortar again and sealed in Pt crucibles sized Φ10 mm × 100 mm.

A detailed procedure for $LiYF_4$ single crystals was described elsewhere[14]. The as-grown crystals were cut into several pieces and then well-polished to ~2.0 mm thickness. The samples are very transparent and one of them (TE0) is shown in the inset of Fig. 1.

The concentrations of the active ions in the samples were measured by inductively coupled plasma–atomic emission spectroscopy (ICP–AES, PerkinElmer Inc., Optima 3000) and the designated symbols for these samples and doping concentrations of rare earths are listed in Table 1. An XD-98X diffractometer (XD-3) was used to identify the phase composition of the single crystal. The absorption spectra ranging from 300 to 600 nm were recorded with a Cary 5000 UV/visible/near-IR (NIR) spectrophotometer (Agilent). The luminescence properties of the crystals were characterized by the excitation and emission spectra measured on an F-4500 spectrophotometer (Hitachi High-Technologies). All measurements were executed at room temperature (RT).

Figure 1 displays the powder x-ray diffraction (XRD) pattern of the sample TE0 and the standard pattern of the $LiYF_4$ crystal (Joint Committee on Powder Diffraction (JCPD) No. 77-0816)[15]. The corresponding lattice plane indexes are also labeled in Fig. 1. The diffraction peaks of $LiYF_4$ single crystals co-doped with Tb^{3+}/Eu^{3+} correspond well to those of standard $LiYF_4$ and have no visible shift compared with standard card JCPD No. 77-0816, indicating that the obtained doped crystal has a pure phase. The other samples also showed similar

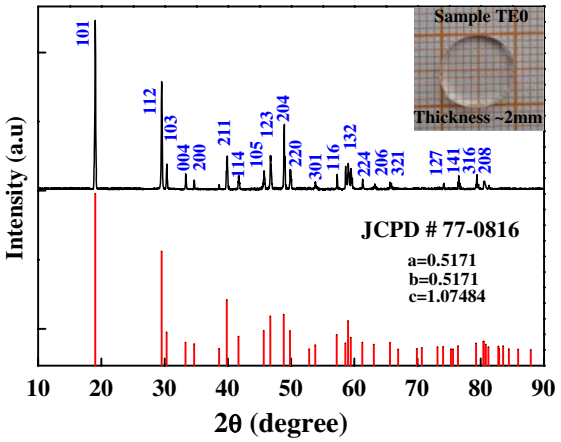

Fig. 1. Powder XRD pattern of Tb^{3+}/Eu^{3+} co-doped $LiYF_4$ crystal (TE0). The standard pattern of the $LiYF_4$ crystal is shown. Inset, $LiYF_4$ single crystal (TE0).

Table 1. Concentrations of Tb^{3+} and Eu^{3+} Ions in $LiYF_4$ Single Crystals[a]

Symbols	T0	TE0	TE1	TE2	TE3	TE4
Tb	0.85	0.84	0.95	1.10	1.11	1.11
Eu	0	0.60	0.60	0.61	0.75	0.90

[a]In units of mol%.

XRD patterns. It proves that small amount of dopants substituting the positions of Y^{3+} ions do not cause any meaningful change of the crystal structure. It also could be obtained that the sample TE0 has the scheelite ($CaWO_4$) structure and its lattice constants can be calculated as follows

$$2 - 2\cos 2\theta = \lambda^2[(h/a)^2 + (k/b)^2 + (l/c)^2], \quad (1)$$

where 2θ is the diffraction angle in corresponding lattice plane indexes (h, k, l), which have been marked in Fig. 1. λ is the Cu K_α radiation wavelength ($\lambda = 0.15406$ nm), and a, b, and c are the lattice constants.

The results are as follows: a = b = 0.5173 nm, and c = 1.0764 nm, which is very close to the standard constants (a = b = 0.5171 nm, and c = 1.07484 nm) shown in Fig. 1.

Figure 2 displays the absorption spectra of Samples T0, TE0, and un-doped $LiYF_4$ crystals which are marked a, b, and c, respectively, ranging from 300 to 600 nm. Obviously, an un-doped $LiYF_4$ single crystal has no visible absorption peaks. It can be seen that at the Tb^{3+} singly doped T0 sample, the main absorption peaks are at ~352, ~358, ~369, ~377, and ~486 nm, which correspond to Tb^{3+} transitions from the $^7F_6$ ground state to the $^5G_5$, $^5L_{10}$, $^5G_6$, $^5D_3$, and $^5D_4$ excited states. With respect to the Tb^{3+}/Eu^{3+} co-doped TE0 sample, obviously additional peaks at ~319 and ~394 nm, which are ascribed to the Eu^{3+} ion transitions from the $^7F_0$ to the $^5H_4$ and $^5L_6$ excited states, appeared. All the corresponding transitions have been clearly marked in Fig. 2. The absorption spectrum of Sample TE0 shows that the crystal co-doped with Tb^{3+}/Eu^{3+} ions can be excited simultaneously efficiently by UV light.

In order to investigate the luminescence properties of a Tb^{3+}/Eu^{3+} co-doped $LiYF_4$ single crystal, the emission spectra of Samples T0 and TE0 under 374 nm excitation were measured and are displayed in Fig. 3. As shown in Fig. 3, the crystal TE0 can emit blue light around 413 and 436 nm, corresponding to $^5D_3 \rightarrow {}^7F_J$ (J = 5, 4) transitions

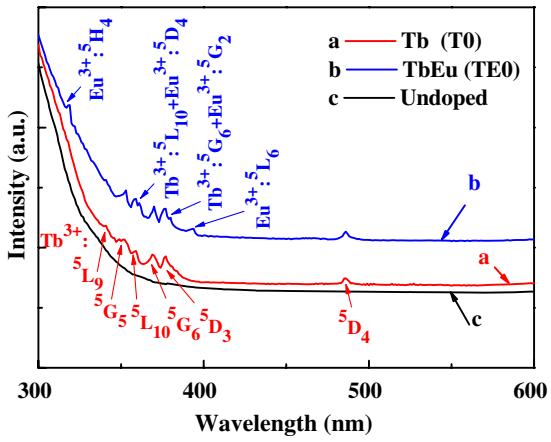

Fig. 2. Absorption spectra of Samples T0 and TE0, and the un-doped crystals (marked a, b, and c, respectively).

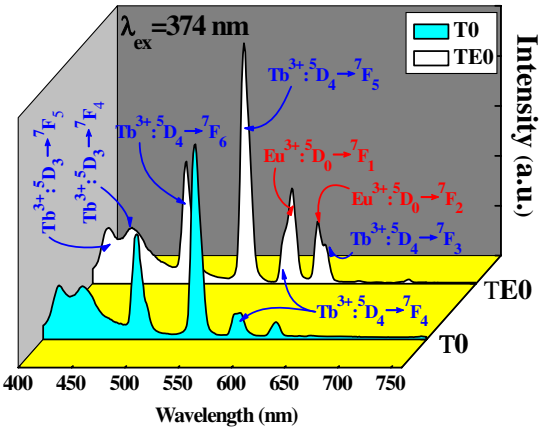

Fig. 3. Emission spectra of Samples T0 and TE0 under 374 nm excitation.

of Tb^{3+}; a green–blue light near 487 nm, due to the electronic transition of Tb^{3+} ($^5D_4 \rightarrow {}^7F_6$); a green light near 542 nm (Tb^{3+}:$^5D_4 \rightarrow {}^7F_5$); an orange light near 587 nm, which originates from the co-contribution of Tb^{3+} and Eu^{3+} due to the overlapped emissions corresponding to the $^5D_4 \rightarrow {}^7F_4$ transition of Tb^{3+} ions and the $^5D_0 \rightarrow {}^7F_1$ transition of Eu^{3+} ions; and a red light near 611 and 618 nm, ascribed to the transitions of Eu^{3+} ($^5D_0 \rightarrow {}^7F_2$) and Tb^{3+} ($^5D_4 \rightarrow {}^7F_3$) ions, respectively. All the transitions are labeled clearly in Fig. 3. The simultaneous emissions of blue, green, and red light enable white light to be possible from Tb^{3+}/Eu^{3+} co-doped $LiYF_4$ crystals pumped by UV light.

Figure 4 presents the excitation spectra of Sample TE0 monitored at 487, 542, and 611 nm wavelengths ranging from 300 to 400 nm for obtaining an optimal excitation wavelength. The monitored spectra are named d, e, and f in Fig. 4, correspondingly. It can be obviously found that the intensity of the excitation peaks for Curve e is slightly stronger than that for Curve d. It indicates that the intensity of the emission peak at 542 nm is slightly stronger than that at 487 nm when excited by corresponding excitation wavelengths. The excitation spectrum for Curve f shows similar characteristic bands of Eu^{3+} ions centering at 306, 318, 360, 380, and 394 nm, and its corresponding electronic transitions from the ground state $^7F_0$ to excited states $^3P_0$, $^5H_4$, $^5D_4$, $^5G_2$, and $^5L_6$, respectively. Four excitation bands peaking at 302 ($^7F_6 \rightarrow {}^5H_6$), 318 ($^7F_6 \rightarrow {}^5H_7$, $^5D_0$), 353 ($^7F_6 \rightarrow {}^5G_5$, $^5D_2$, $^5G_4$, $^5L_9$, $^5G_3$, $^5L_8$), and 374 nm ($^7F_6 \rightarrow {}^5D_3$, $^5L_{10}$) are included in the excitation spectrum of Tb^{3+} for Curve d. Moreover, Curve e shows the similar excitation spectrum to Curve d. As shown in Fig. 4, the excitation wavelengths at 353, 362, 374, and 384 nm were chosen to obtain a better white light emission. Figure 5 shows the emission spectra of Sample TE0 ranging from 400 to 760 nm under the excitation wavelengths 353, 362, 374, and 384 nm, respectively. When excited by those wavelengths, the emission spectra show similar bands while the luminous intensities are changed with the excitation wavelengths. The related electronic transitions have been discussed previously in the context of Fig. 3.

The different concentrations of dopants in $LiYF_4$ single crystals were prepared for obtaining an optimum white light emission. Figure 6 displays the fluorescence spectra of the samples TEi ($i = 0$–4) under 384 nm excitation wavelength. It can be clearly found that the emission

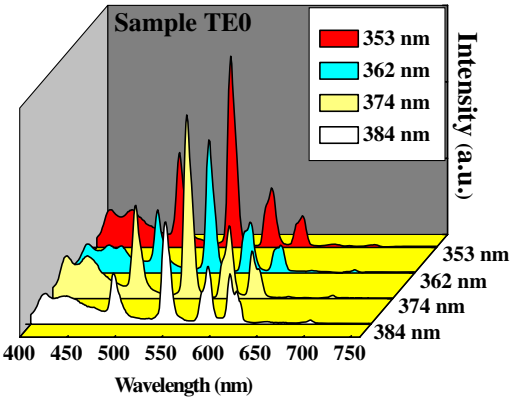

Fig. 5. Emission spectra of Sample TE0 under various excitation wavelengths (353, 362, 374, and 384 nm).

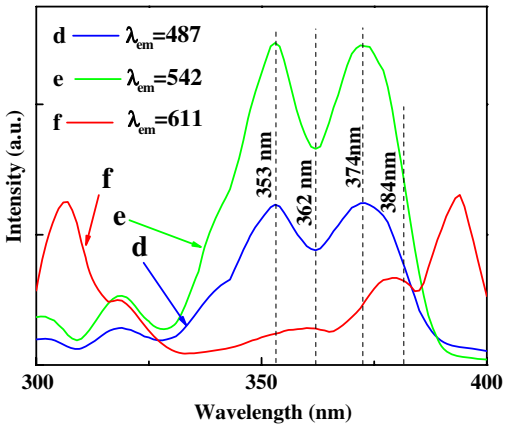

Fig. 4. Excitation spectra of Sample TE0 monitored at 487, 542, and 611 nm wavelengths.

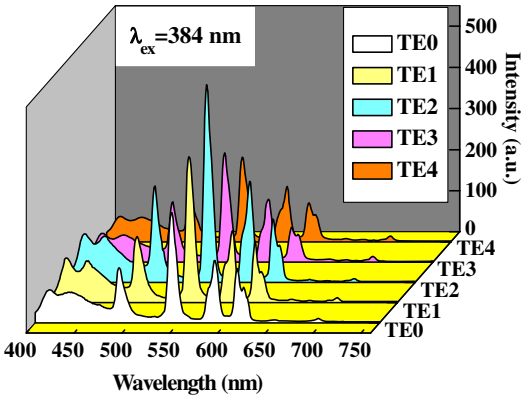

Fig. 6. Emission spectra of various Tb^{3+}/Eu^{3+} co-doped $LiYF_4$ crystals under 384 nm excitation.

peaks of the samples are similar with a slight difference in luminous intensities. One can state that emission intensities change with concentrations of Tb^{3+} and Eu^{3+} ions in $LiYF_4$ single crystals. This luminous phenomenon implies a complicated process of energy transition between the Tb^{3+} and Eu^{3+} ions in the host material[12].

It is necessary to mark chromaticity coordinates of the samples on a standard chromaticity diagram for reflecting their luminescence color which is shown in Fig. 7. The chromaticity coordinates for the emissions of the samples TEi ($i = 0$–4) under 384 nm excitation wavelengths can be calculated using the following[16]

$$x = \frac{X}{X+Y+Z}, \qquad y = \frac{Y}{X+Y+Z}, \qquad z = \frac{Z}{X+Y+Z}, \tag{2}$$

where X, Y, and Z are three tristimulus values. Those three values are given by the following[16]

$$X = \int_\lambda P(\lambda)\bar{x}(\lambda)\mathrm{d}\lambda, \qquad Y = \int_\lambda P(\lambda)\bar{y}(\lambda)\mathrm{d}\lambda, \qquad Z = \int_\lambda P(\lambda)\bar{z}(\lambda)\mathrm{d}\lambda, \tag{3}$$

where λ is the wavelength of the equivalent monochromatic light. $P(\lambda)$ is the spectral power distribution, which is the input for tristimulus values and its data are shown in Fig. 6. $\bar{x}(\lambda)$, $\bar{y}(\lambda)$, and $\bar{z}(\lambda)$ are the three color-matching functions.

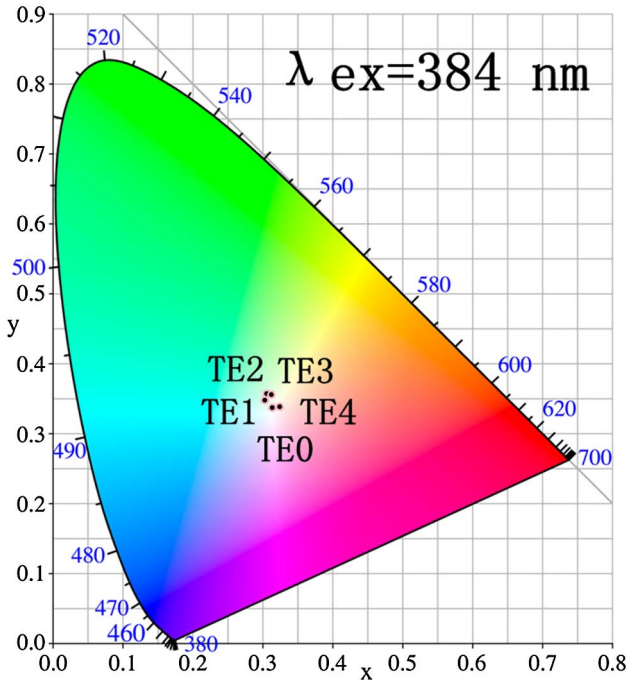

Fig. 7. CIE chromaticity coordinates diagram for Samples TEi ($i = 0$–4) under 384 nm excitation.

Color temperature (T_c) is also a key technical factor for evaluating the applicability of a luminescence material. It can be estimated using McCamy's equation

$$T_c = 449n^3 + 3525n^2 + 6823.3n + 5520.33, \quad \text{where } n = \frac{(0.23881)R + (0.25499)G + (-0.58291)B}{(0.11109)R + (-0.85406)G + (0.52289)B}, \tag{4}$$

where R, G, and B are the spectral matching stimulus which can be calculated by Matrix

$$\begin{pmatrix} X \\ Y \\ Z \end{pmatrix} = \begin{pmatrix} -0.14282 & 1.54924 & -0.95641 \\ -0.32466 & 1.57837 & -0.73191 \\ -0.68202 & 0.77073 & 0.56332 \end{pmatrix} \begin{pmatrix} R \\ G \\ B \end{pmatrix}, \tag{5}$$

where X, Y, and Z are three tristimulus values which can be calculated as per Eqs. (2) and (3).

The color render index (R_a) and color quality scale (Q_a) are widely used for assessing the luminescence performance of a light source. Thus, introduction of these parameters is good for investigating the luminescence performance of the samples' TEi ($i = 0$–4). Detailed procedures for the calculation of R_a and Q_a are available in Refs. [17,18]. The final calculations for these are provided as follows

$$R_a = \frac{1}{8}\sum_{i=1}^{8}(100 - 4.6\Delta E_i), \tag{6}$$

where ΔE_i is the difference in color appearance for each sample between illumination by the test source and the reference illuminant which can be computed in Commission Internationale de L'Eclairage (CIE) $W^*U^*V^*$ uniform color space

$$Q_a = 10\,\mathrm{ln}(\exp((100 - 3.1 \times \Delta E_{\mathrm{rms}})/10) + 1), \tag{7}$$

where ΔE_{rms} is the rms of the 15 color differences for each sample illuminated by the test source and reference illuminant. Note that the Q_a can be calculated by using Eq. (7) when the correlated color temperature of the test light source is greater than 3500 K.

The chromaticity coordinates of the TEi ($i = 0$–4) under 384 nm excitation were calculated using Eq. (2) and are marked in a chromaticity diagram as shown in Fig. 7. It can be seen that emission intensities of the samples are all in the white light region, and the emission of Sample TE4 is much closer to the standard equal energy white light illumination ($x = 0.333$, $y = 0.333$). To further understand the luminous characteristic of these samples, the luminous parameters, including chromaticity coordinates, color temperature (T_c), color rendering index (R_a), and color quality scale (Q_a), which were calculated using Eqs. (2)–(7), are listed in Table 2. Although the luminous properties of these samples fall into the white light region, more effort should focus on decreasing the color

Table 2. Luminous Parameters of Samples TEi[a]

	Luminous Parameters				
Samples	CIE(x, y)		T_c (K)	R_a	Q_a
TE0	0.3130	0.3377	6441	76	75
TE1	0.3027	0.3480	6904	68	60
TE2	0.3051	0.3577	6713	64	66
TE3	0.3120	0.3555	6399	70	67
TE4	0.3242	0.3389	5878	77	75

[a]$i = 0$–4.

temperature and increase the color quality scale of Tb^{3+}/Eu^{3+} co-doped $LiYF_4$ crystals, which is relegated to future work.

In conclusion, $LiYF_4$ single crystals co-doped with Tb^{3+}/Eu^{3+} for LEDs are obtained by a modified Bridgman method. It shows better luminescent properties from the emission spectra including synchronously blue, green, and red light bands. This work proves that white light emission from $LiYF_4$ crystals co-doped with Tb^{3+}/Eu^{3+} ions can be achieved under a proper excitation wavelength. Furthermore, all the results indicate that the emission light color can be tuned for different demands by varying the excitation wavelengths or adjusting the concentrations of Tb^{3+}/Eu^{3+} ions in $LiYF_4$ single crystals. Due to excellent advantages of white light-emitting crystals, $LiYF_4$ crystals co-doped with Tb^{3+}/Eu^{3+} ions might have broad application prospects for white light emission.

This work was supported in part by the National Natural Science Foundation of China (Nos. 51472125 and 51272109) and the K. C. Wong Magna Fund in Ningbo University.

References

1. E. F. Schubert and J. K. Kim, Science **308**, 1274 (2005).
2. N. Kimura, K. Sakuma, S. Hirafune, K. Asano, N. Hirosaki, and R. J. Xie, Appl. Phys. Lett. **90**, 051109 (2007).
3. L. Tang, H. P. Xia, P. Y. Wang, J. T. Peng, Y. P. Zhang, and H. C. Jiang, J. Mater. Sci. **48**, 7518 (2013).
4. R. G. Ye, Z. G. Cui, Y. J. Hua, D. G. Deng, S. L. Zhao, C. X. Li, and S. Q. Xu, J. Non-Cryst. Solids **357**, 2282 (2011).
5. Z. Y. Lin, X. L. Liang, Y. W. Ou, C. X. Fan, S. L. Yuan, H. D. Zeng, and G. R. Chen, J. Alloy. Compd. **496**, L33 (2010).
6. Z. F. Zhu, Y. B. Zhang, Y. P. Qiao, H. Liu, and D. G. Liu, J. Lumin. **134**, 724 (2013).
7. Y. Yu, F. Song, C. G. Ming, J. D. Liu, W. Li, Y. L. Liu, and H. Y. Zhao, Opt. Commun. **303**, 62 (2013).
8. X. R. Hou, S. M. Zhou, T. T. Jia, H. Lin, and H. Teng, J. Alloy. Compd. **509**, 2793 (2011).
9. L. J. Ren, X. H. Lei, X. Q. Du, L. Jin, W. M. Chen, and Y. A. Feng, J. Lumin. **142**, 150 (2013).
10. J. Yang, B. J. Chen, E. Y. B. Pun, B. Zhai, and H. Lin, J. Lumin. **134**, 622 (2013).
11. S. L. Zhao, F. X. Xin, S. Q. Xu, D. G. Deng, L. H. Huang, H. P. Wang, and Y. J. Hua, J. Non-Cryst. Solids **357**, 2424 (2011).
12. C. F. Zhu, S. Chaussedent, S. J. Liu, Y. F. Zhang, A. Monteil, N. Gaumer, and Y. Z. Yue, J. Alloy. Compd. **555**, 232 (2013).
13. L. Tang, H. Xia, P. Wang, J. Peng, Y. Zhang, and H. Jiang, Chin. Opt. Lett. **11**, 061603 (2013).
14. Q. Fang, H. Chen, F. Xu, S. Wang, Z. Liang, and C. Jiang, Chin. Opt. Lett. **8**, 1071 (2010).
15. S. Li, P. Wang, H. Xia, J. Peng, L. Tang, Y. Zhang, and H. Jiang, Chin. Opt. Lett. **12**, 021601 (2014).
16. R. J. Mortimer and T. S. Varley, Displays **32**, 35 (2011).
17. L. Fu, H. P. Xia, Y. M. Dong, S. S. Li, X. M. Gu, H. C. Jiang, and B. J. Chen, IEEE Photonic. Tech. Lett. **26**, 1485 (2004).
18. W. Davis and Y. Ohno, Opt. Eng. **49**, 033602 (2010).